Proceedings of the 9ICEG
9th International Congress on Environmental Geotechnics
25-28 June, 2023 | Chania, Greece
© Authors: All rights reserved, 2023
https://doi.org/10.53243/ICEG2023-46

Immobilizing of Lead and Copper in Aqueous Solution Using Microbial- and Enzyme-induced Carbonate Precipitation

W.C. Cheng[1,2], L. Wang[2,3], Z.F. Xue[2,3], M.M. Rahman[4], Y.X. Xie[2,3] and W. Hu[2,3]

[1] *Professor, School of Civil Engineering, Xi'an University of Architecture and Technology, Xi'an, China, email: w-c.cheng@xauat.edu.cn*

[2] *Shaanxi Key Laboratory of Geotechnical and Underground Space Engineering (XAUAT), Xi'an, China*

[3] *PhD student, School of Civil Engineering, Xi'an University of Architecture and Technology, Xi'an, China, email: wanglin@xauat.edu.cn (L. Wang), xuezhongfei@xauat.edu.cn (Z-F. Xue), xieyixin@xauat.edu.cn (Y-X. Xie), wenlehu@xauat.edu.cn (W. Hu),*

[4] *Professor, UniSA STEM, ScaRCE, University of South Australia, SA 5000, Australia, email: mizanur.rahman@unisa.edu.au*

ABSTRACT

Inappropriate irrigation could trigger migration of heavy metals into surrounding environments, causing their accumulation and a serious threat to human central nervous system. Traditional site remediation technologies are criticized because they are time-consuming and costly. In the past few years, the microbial-induced carbonate precipitation (MICP) is deemed as an alternative to traditional technologies due to its easy maneuverability. The enzyme-induced carbonate precipitation (EICP) has attracted attention as bacterial cultivation is waived before catalyzing urea hydrolysis. The present work applied MICP and EICP technologies to the lead (Pb) and copper (Cu) immobilization. The effect of the degree of urea hydrolysis, mass and species of carbonate precipitation, and chemical and thermodynamic properties of carbonates on the immobilization efficiency was investigated. Results showed that NH_4^+ concentration reduced when subjected to the effect of Pb^{2+} or Cu^{2+} toxicity, and for a given Pb^{2+} or Cu^{2+} concentration, it was much higher under MICP than under EICP. Further, the immobilization efficiency against Cu^{2+} is way below that against Pb^{2+}. The reduction in the immobilization efficiency against Pb^{2+} and Cu^{2+} appeared to be due to two precipitates respectively (i.e., cotunnite and atacamite). Their chemical and thermodynamic properties were not as good as those of calcite, cerussite, phosgenite, and malachite. Their degradation, when subjected to harsh pH conditions, results in a reduction in the immobilization efficiency.

Keywords: lead, copper, immobilization efficiency, thermodynamic properties

1 INTRODUCTION

Transforming heavy metals from a solid phase to a liquid phase by their mobility or solubility increases notably their bioavailability. To this end, immobilising of heavy metals is deemed crucial in securing the safety of surrounding environments and human health (Wang et al., 2022a,b; Xue et al., 2022). Soil flushing (Dermont et al., 2008; Zhu et al., 2021), electrokinetic remediation (Lockhart, 1983; Mena et al., 2015), chemical precipitation (Gong et al., 2020; Khan et al., 2004), ion exchange (Aparicio et al., 2021; Hamby, 1996), and phytoremediation (Jalali et al., 2007; Zine et al., 2020) have been widely applied to tackle the raised issue. Despite that, the traditional technologies are often criticized because they are costly and can impose risks of secondary pollution (Bhattacharya et al., 2018).

Biologically controlled mineralization and biologically induced mineralization are the most common methods of biomineralization. The microbial-induced carbonate precipitation (MICP) (Castanier et al., 1993; Phillips et al., 2016) and enzyme-induced carbonate precipitation (EICP) (Maubois, 1984; Larsen et al., 2008; Moghal et al., 2020) belong to the latter. *Sporosarcina pasteurii* due to its extremely high activity has extensively been used as ureolytic bacteria for catalysing urea hydrolysis. There are three inherent mechanisms that play a major part in the biomineralization process, including abiotic precipitation, biosorption, and biotic precipitation. It is well acknowledged that the abiotic precipitation

could badly degrade the immobilization efficiency because of its low thermodynamic stability (Benson & Teague, 1980; Robie & Hemingway, 1995). Further, the higher the degree of urea hydrolysis, the more the carbonate ions precipitated with heavy metals, and the higher the immobilization efficiency (Achal et al. 2012; Xue et al. 2022). However, Duarte-Nass et al. (2020) found that a low immobilization efficiency against Cu also appears with high degree of ureolysis. Moreover, considering Ca^{2+} forms competitive adsorption with heavy metal ions, the ureolytic bacteria bind preferentially themselves with Ca^{2+}, indicating an enhancement of the resistance against heavy metal ions (Wang et al., 2022a,b).

On the other hand, enzymes are more environmentally adaptive when compared to microorganisms that require appropriate environments for living and supply of oxygen and nutrients. Nanometer-sized enzymes are much smaller than micrometer-sized microorganisms, and therefore, they can penetrate the deeper grounds with no difficulty when applied to 'in-situ' conditions. Li et al. (2022) explored the inherent mechanisms affecting the retention of Cd^{2+}. Cd^{2+} were immobilised with otavite ($CdCO_3$), calcite co-precipitation ($CaCO_3$-Cd), and vaterite/aragonite chemisorption ($CaMg(CO_3)_2$). Despite that, the above analysis reveals several research gaps that remain to be addressed. The main objectives of this study are: (1) to conduct a comparison of the degree of urea hydrolysis, and mass and species of carbonate precipitation between MICP and EICP, (2) to investigate the chemical and thermodynamic properties of precipitated carbonates, and (3) to explore the underlying mechanisms affecting the Pb and Cu immobilization by MICP and EICP respectively.

2 MATERIALS AND METHODS

2.1 MICP: bacteria and cultivation

The use of *Sporosarcina pasteurii* in a freeze-dried form aimed to catalyse urea hydrolysis. The strain of 0.1 ml was transferred to a 100 ml liquid medium composed of NH_4Cl of 10 g/L, urea of 20 g/L, yeast extract of 10 g/L, $MnSO_4 \cdot H_2O$ of 10 mg/L, and $NiCl \cdot 6H_2O$ of 24 mg/L for their cultivation at 30°C and at 180 rpm for 24 hrs. The chemicals are analytically pure. Further, pH of the bacteria resuscitation environment being 8.8 was measured using a benchtop pH meter (HI2003; HANNA Instruments Inc., Italy). The bacterial solution was mixed with glycerol using a 7:3 ratio and stored at -20°C for future use.

The biomass (OD_{600}) and urease activity (UA) were measured for 172 h through the activated ureolytic bacteria when subjected to pH values of 6, 8, 8.8, and 10 respectively. OD_{600} was measured by a visible light spectrophotometer. The measurement of UA was on a basis of the ureolysis rate and referred to the method recommended by Whiffin et al. (2007); 2 ml reaction solution is mixed with 18 ml 1.11 M urea and the electrical conductivity (EC) is measured at 0 and 5 min by a benchtop conductivity meter. Eq. 1 shows the equation applied to UA evaluation.

$$UA = \frac{EC_5 - EC_0}{5} \times 10 \times 1.11 \ (\text{mM urea hydrolysed/min}) \quad (1)$$

where EC_0 and EC_5 are the electrical conductivity at 0 and 5 min respectively.

2.2 MICP: test tube experiments

In the present work, MICP was attained through a series of test tube experiments and applied to the removal of Pb and Cu. The OD_{600} curve determined how long did the cultivation take the ureolytic bacteria to achieve their highest activity. The blank OD_{600} was measured to be 0.045 prior to the use of the bacterial solution. As recommended by Duarte-Nass et al. (2020), 0.33 M is considered as the minimum urea concentration that is required to promote the ureolytic bacteria to grow and reproduce. 0.5 M urea concentration was, therefore, adopted herein. Fang et al. (2021) suggested that to secure the immobilization efficiency, the concentration of calcium source is supposed to be at least five times higher than the contaminant concentration, thereby preventing the instability of the carbonate precipitation. Given a maximum of 50 mM applied to Pb^{2+} or Cu^{2+} concentration, the concentration of calcium source was thus set to 0.25 M. Upon the completion of bacterial cultivation, the bacterial solution with OD_{600} values falling within a 1.8-2.1 range was inoculated (10% (v/v)) into the liquid medium containing $Pb(NO_3)_2$ or $Cu(NO_3)_2$ at concentrations varying in a 0-50 mM range, 0.5 M urea, 0.25 M $CaCl_2$, and 2g/L yeast extract. In the present work, three replicates were considered for each test set. EC, pH, and UA measurements were carried out at 0, 4, 12, 24, 48 hrs respectively. Each measurement

used a 2 ml sample. While OD_{600} was measured at 12, 24, 48 hrs respectively. Although NH_4^+ was one of the harmful by-products produced in the biomineralization process, they represented the degree of urea hydrolysis. To this end, NH_4^+ were measured using Nessler's reagent colorimetric method (Whiffin et al., 2007). In addition to NH_4^+, the precipitation mass tended to be introduced as well for assessing the activity of the urease. Furthermore, Pb^{2+} or Cu^{2+} concentration was measured through an atomic spectrophotometer. The immobilization efficiency can be evaluated via the equation below:

$$\text{Immobilization efficiency} = \frac{C_0 - C_1}{C_0} \times 100\% \quad (2)$$

where C_0 and C_1 are Pb^{2+} or Cu^{2+} concentration before and after remediation respectively. Table 1 summarizes the scheme applied to the test tube experiments.

2.3 EICP: urease extraction

The use of *Canavalia ensiformis* mainly aimed to extract urease enzyme rather than using commercially available enzymes because they are usually costly. *Canavalia ensiformis* was ground and sieved using a sieve with 150 μm opening. A solution composed of grounded *Canavalia ensiformis* and ethanol was centrifuged at 8000 rpm for 0.5 h and then stored at 4°C for 4 h. The supernatant extracted from the solution was centrifuged again at 4000 rpm for 1 h and the precipitate (i.e., urease) was stored at -20°C. Nessler's reagent colorimetric method was applied to measure NH_4^+ concentration (Bzura & Koncki, 2019). Prior to the measurement, a calibration line was set up. The absorbance measured using a spectrophotometer was substituted into the calibration line to determine NH_4^+ concentration. The urease activity was calculated as 5.06 mM urea hydrolyzed/min (Whiffin et al. 2007).

2.4 EICP: test tube experiments

The test tube experiments were composed of four main phases: (1) adding urea, (2) adding $Pb(NO_3)_2$ or $Cu(NO_3)_2$, (3) adding calcium source, and (4) adding urease enzyme. Measurements undertaken in the test tube experiments included pH, EC, UA, NH_4^+ concentration, and precipitation mass. Their frequency of measurement is summarized also in the same figure. Table 1 summarizes the scheme applied to the test tube experiments. All test tube experiments were performed under the same testing conditions to prevent interferences induced by external factors.

Table 1. *Testing scheme applied to Pb and Cu immobilization*

Contamination concentration (mM)		$CaCl_2$ concentration (mM)	Urea concentration (mM)	OD_{600}	Urease concentration (g/L)
Pb	5, 10, 30, 40, 50	250	500	1.8-2.1	3
		/	500	1.8-2.1	3
Cu	5, 10, 30, 40, 50	250	500	1.8-2.1	3
		/	500	1.8-2.1	3

Note: OD_{600} is only applicable under MICP.

2.5 Biomineralization simulation

The species and sequence of carbonate precipitation was not revealed by the test tube experiments but by the numerical simulation using the Visual MINTEQ software. The urea hydrolysis was reproduced in accordance with the ratio of NH_4^+ to CO_3^{2-} being 2:1 (Gat et al., 2017) despite the omittance of bacterial cultivation and inoculation. In case CO_3^{2-} does not play part in the biomineralization process, such a carbonate precipitation is classed as 'abiotic' precipitation (e.g. $PbCl_2$). In contrast, it is classified as 'biotic' precipitation (e.g. $PbCO_3$). It is well acknowledged that abiotic precipitation due to its higher solubility product has a thermodynamic stability much lower than biotic precipitation, meaning that the immobilization efficiency could degrade when exposed to harsh pH conditions. Considering NH_4^+ and CO_3^{2-} were crucial in determining the degree of urea hydrolysis and whether the degree of urea hydrolysis is high enough to produce biotic precipitation, their concentrations were extracted upon the completion of urea hydrolysis as input parameters in the proposed numerical simulation (see Table 2).

Table 2. *Summary of the input parameters applied to the numerical simulations*

Contamination concentration (mM)		NH_4^+ concentration (mM)	CO_3^{2-} concentration (mM)	$CaCl_2$ concentration (mM)	NH_4Cl concentration (mM)
Pb	5, 10, 20, 30, 40, 50, 60, 70, 80, 90, 100	10, 30, 50, 70, 90, 110, 200	5, 15, 25, 35, 45, 55, 100	250	18.7
		10, 30, 50, 70, 90, 110, 200	5, 15, 25, 35, 45, 55, 100	/	18.7
Cu	5, 10, 20, 30, 40, 50, 60, 70, 80, 90, 100	10, 30, 50, 70, 90, 110, 200	5, 15, 25, 35, 45, 55, 100	250	18.7
		10, 30, 50, 70, 90, 110, 200	5, 15, 25, 35, 45, 55, 100	/	18.7

Note: NH_4Cl addition is only considered in the numerical simulations under MICP.

3 RESULTS AND DISCCUSION

3.1 Effect of degree of urea hydrolysis

Figure 1 shows the relationships of NH_4^+ concentration versus Pb^{2+} or Cu^{2+} concentration under MICP and EICP respectively. NH_4^+ concentration decreases with the increasing Pb^{2+} or Cu^{2+} concentration, meaning that the more significant the effect of Pb^{2+} or Cu^{2+} toxicity, the lower the urease activity, and the lower the degree of urea hydrolysis. Further, for a given Pb^{2+} or Cu^{2+} concentration, NH_4^+ concentration under MICP is much higher than that under EICP. UA under MICP is measured being 18.83 mM urea hydrolysed/min, which is about four times higher than UA under EICP (i.e. 5.06 mM urea hydrolysed/min). These results provide testimony supporting the above argument. Moreover, NH_4^+ concentration applied to Pb immobilization is much higher than that applied to Cu immobilization given their same concentration. Compared to Pb^{2+}, Cu^{2+} can denature the urease, causing urease inactivation and reduction in NH_4^+ concentration. Given the ratio of NH_4^+ to CO_3^{2-} being 2:1 (Gat et al., 2017), 100 mM NH_4^+ corresponding to 50 mM CO_3^{2-} is deemed necessary to precipitate 50 mM Pb^{2+} or Cu^{2+}. An immobilization efficiency as high as 100% is attained when 50 mM Pb^{2+} or Cu^{2+} is precipitated. NH_4^+ concentration under EICP is way below 100 mM when even subjected to 5 mM Pb^{2+} or Cu^{2+} concentration (the lowest in this work). In contrast, NH_4^+ concentration under MICP is in great excess of 100 mM when even subjected to 50 mM Pb^{2+} or Cu^{2+} concentration (the highest in this work). The higher NH_4^+ concentration under MICP is most likely due to the higher urease activity. Despite that, the immobilization efficiency depends upon not only the degree of urea hydrolysis but also other influencing factors, such as species of carbonate precipitation. In short, NH_4^+ concentration decreases with the increasing Pb^{2+} or Cu^{2+} concentration. NH_4^+ concentration is much higher under MICP. Compared to the effect of Pb^{2+} toxicity, the effect Cu^{2+} toxicity more significantly depresses the urease activity.

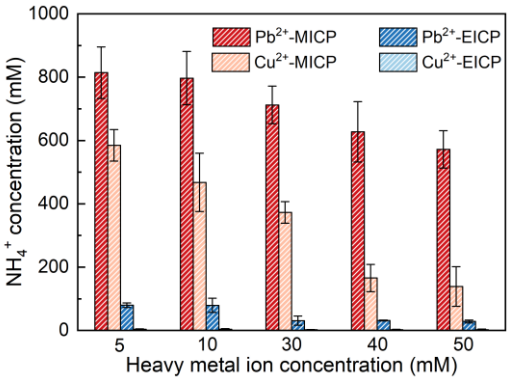


Figure 1. *Relationships of NH_4^+ concentration versus Pb^{2+} or Cu^{2+} concentration under MICP and EICP respectively*

3.2 Pb or Cu immobilization

The relationships of immobilization efficiency and remaining ion versus Pb^{2+} or Cu^{2+} concentration are depicted in Figure 2. Under MICP, the immobilization efficiency of 100% is attained when Pb^{2+}

concentration falls within a 5-50 mM range. Although the degree of urea hydrolysis is quite low, the immobilization efficiency of 100% is also attained under EICP when Pb^{2+} concentration falls within a 5-50 mM range. On the other hand, under MICP, the immobilization efficiency of below 10% is attained when Cu^{2+} concentration falls within a 5-30 mM range. It increases to 77% when subjected to Cu^{2+} concentration at 40 mM and further to 84% when subjected to Cu^{2+} concentration at 50 mM. Under EICP, the immobilization efficiency of higher than 50% is attained when Cu^{2+} concentration falls within a range of 5-10 mM. The immobilization efficiency reduces to approximately 20% when subjected to Cu^{2+} concentration falling within a range of 30-50 mM. In short, MICP performs similarly to EICP in terms of Pb immobilization. Despite that, there is a significant discrepancy in Cu immobilization between MICP and EICP. The immobilization efficiency against Cu^{2+} is not as high as that against Pb^{2+}, and such low immobilization efficiency appears to present in some ranges of NH_4^+ and Cu^{2+} concentration. In light of the above, the impact of the species of carbonate precipitation deserves further exploration.

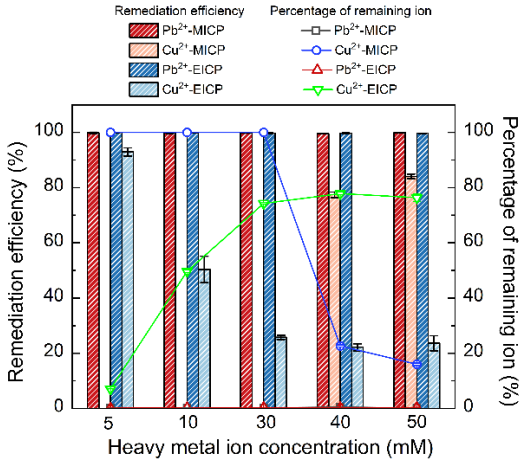


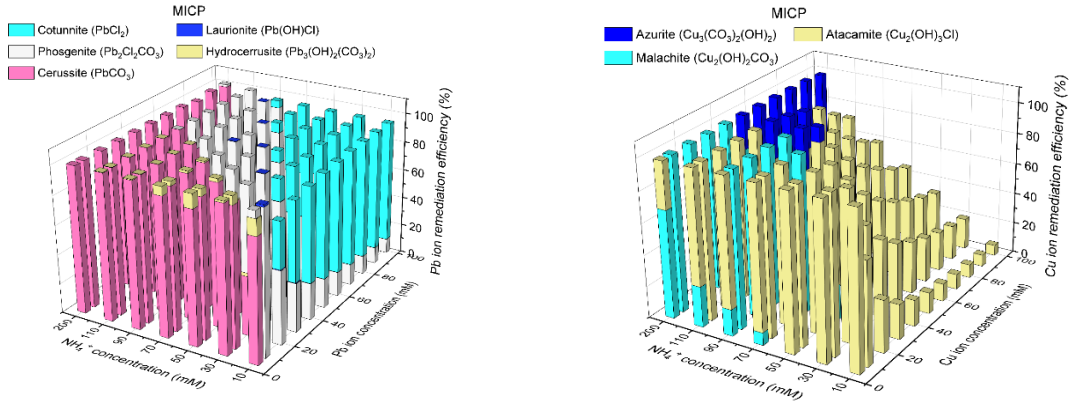
Figure 2. *Relationships of immobilization efficiency and remaining Pb^{2+} or Cu^{2+} versus Pb^{2+} or Cu^{2+} concentration under MICP and EICP respectively*

3.3 Species of carbonate precipitation

The variations of immobilization efficiency versus hydrolyzed urea concentration and Pb^{2+} or Cu^{2+} concentration under MICP are depicted in Figure 3. When subjected to 5 mM $Pb(NO_3)_2$ and 200 mM NH_4^+, 100 mM CO_3^{2-} can precipitate 100 mM Pb^{2+} ($PbCO_3$) much higher than 5 mM Pb^{2+}, indicating a immobilization efficiency of 100% (see Figure 3a). There are four species of carbonate precipitation, including $Pb_2Cl_2CO_3$, Pb(OH)Cl, $Pb_3(CO_3)_2(OH)_2$, and $PbCl_2$, when CO_3^{2-} concentration is not high enough to precipitate Pb^{2+}. 5 mM CO_3^{2-} can only precipitate 10 mM Pb^{2+} ($Pb_2Cl_2CO_3$) when subjected to 50 mM $Pb(NO_3)_2$ and 10 mM NH_4^+, leaving 40 mM Pb^{2+} behind. The remaining 40 mM Pb^{2+} can only be precipitated with Cl^-, reducing the immobilization efficiency by 9%. Also, the reduction in CO_3^{2-} concentration causes a difficulty in securing the immobilization efficiency because Cu immobilization is not attained via biotic precipitation but via abiotic precipitation. For example, when NH_4^+ concentration is reduced sharply from 200 mM to 10 mM and $Cu(NO_3)_2$ concentration is notably elevated from 10 mM to 100 mM, $Cu_2CO_3(OH)_2$ is transformed to $Cu_2(OH)_3Cl$, causing a reduction of the immobilization efficiency by 93.3% (see Figure 3b). Despite that, the other two species of precipitation ($Cu_3(CO_3)_2(OH)_2$ and $Cu_2(OH)_2CO_3$) are present when CO_3^{2-} concentration is high enough. $Cu_2(OH)_2CO_3$ is precipitated when subjected to 10 mM $Cu(NO_3)_2$ and 200 mM NH_4^+.100 mM CO_3^{2-} can precipitate 200 mM Cu^{2+} much higher than 10 mM Cu^{2+}, indicating a immobilization efficiency of 100%. Note that for the test tube experiments, more than 400 mM NH_4^+ are hydrolysed when subjected to Cu^{2+} concentration falling in a 5-30 mM range, but such high NH_4^+ concentration corresponds to a immobilization efficiency close to zero (see Figures 1 and 2). Although NH_4^+ concentration higher than 400 mM is not within the scope of the numerical simulation, the immobilization efficiency close to zero is most likely due to the fact that NH_4^+ concentration higher than 400 mM raises pH to above 9, and such strongly alkaline environments promote the formation of copper-ammonia complex with a chemical formula of $[Cu(NH_3)_4(H_2O)_2]^{2+}$ (Duarte-Nass et al., 2020). The copper-ammonia complex turns Cu^{2+} into a free state, degrading the immobilization efficiency.

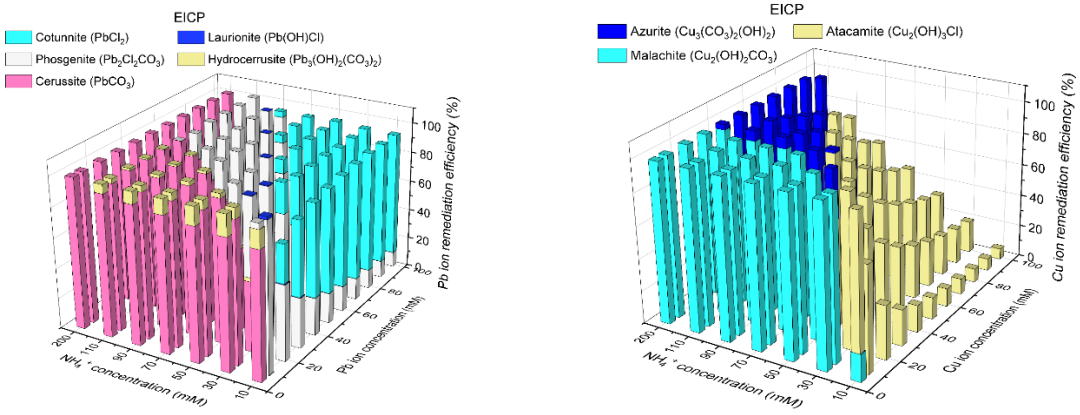
The variations of immobilization efficiency versus hydrolyzed urea concentration and Pb^{2+} or Cu^{2+} concentration under EICP are shown in Figure 4. When subjected to 5 mM $Pb(NO_3)_2$ and 200 mM NH_4^+, 100 mM CO_3^{2-} can precipitate 100 mM Pb^{2+} ($PbCO_3$) much higher than 5 mM Pb^{2+}, corresponding to a

immobilization efficiency of 100% (see Figure 4a). $PbCl_2$, $Pb(OH)Cl$, $Pb_2Cl_2CO_3$, and $Pb_3(OH)_2(CO_3)_2$ are precipitated when CO_3^{2-} concentration is not high enough. $PbCO_3$, when subjected to 100 mM $Pb(NO_3)_2$ and 10 mM NH_4^+, is transformed to $PbCl_2$ and $Pb_2Cl_2CO_3$ because 5 mM CO_3^{2-} can only precipitate 10 mM Pb^{2+} ($Pb_2Cl_2CO_3$), leaving 90 mM Pb^{2+} to be precipitated with Cl^-. The formation of $PbCl_2$ reduces the immobilization efficiency by about 8%. As to Cu immobilization, $Cu_2(OH)_2CO_3$ could be transformed to $Cu_3(CO_3)_2(OH)_2$ and $Cu_2(OH)_3Cl$ when the degree of urea hydrolysis is high enough. Given 100 mM $Cu(NO_3)_2$ and 10 mM NH_4^+, the formation of $Cu_2(OH)_3Cl$ leads to a substantial reduction in the immobilization efficiency by 93.3% (see Figure 4b). In contrast, 100 mM CO_3^{2-} can precipitate 200 mM Cu^{2+} ($Cu_2(OH)_2CO_3$) when subjected to 5 mM $Cu(NO_3)_2$ and 200 mM NH_4^+, meaning that a majority of Cu^{2+} is precipitated. These results lead us to summarize that the immobilization efficiency against Pb^{2+} or Cu^{2+} could not only be influenced by the degree of urea hydrolysis but by the species of carbonate precipitation. The low degree of urea hydrolysis leads to low CO_3^{2-} concentration, promoting the formation of abiotic precipitation, such as $PbCl_2$ and $Cu_2(OH)_3Cl$. They degrade notably the immobilization efficiency.



(a) (b)

Figure 3. *(a) variations of immobilization efficiency against hydrolyzed urea concentration and Pb^{2+} concentration under MICP and (b) variations of immobilization efficiency against hydrolyzed urea concentration and Cu^{2+} concentration under MICP*



(a) (b)

Figure 4. *(a) variations of immobilization efficiency against hydrolyzed urea concentration and Pb^{2+} concentration under EICP and (b) variations of immobilization efficiency against hydrolyzed urea concentration and Cu^{2+} concentration under EICP*

3.4 Chemical and thermodynamic properties of carbonates

Chemical stability for carbonate precipitations under harsh pH conditions is deemed crucial in securing immobilization efficiency. The variation of pH against Pb^{2+} and Cu^{2+} under MICP and EICP considering the hydrolysed urea concentrations varying in a 10-200 mM range is depicted in Figures 5 and 6 respectively. pH, while remedying Pb^{2+} using MICP, reduces from 7 to 5 (see Figure 5a). Higher NH_4^+ concentrations delay such reduction in pH when Pb^{2+} concentration goes up. pH remains at some 7 when NH_4^+ concentration reaches 200 mM. pH, while remedying Cu^{2+} using MICP, reduces from 6 to 4

(see Figure 5b). Similarly, higher NH_4^+ concentrations put off such reduction in pH as Cu^{2+} concentration goes up. While remedying Cu^{2+}, pH being approximately 6 is attained as NH_4^+ concentration reaches 200 mM. When subjected to such harsh pH conditions, carbonate precipitation of low chemical stability, induced by MICP, may dissolve or degrade (Benson & Teague, 1980; Robie & Hemingway, 1995). Lower degrees of urea hydrolysis could aggravate the dissolution or degradation of carbonate precipitation. On the other hand, while remedying Pb^{2+} using EICP, pH decreases from 7 to 5 (see Figure 6a). Further, pH decreases from 6 to 4 while remedying Cu^{2+} using EICP (see Figure 6b). It can also be seen that higher NH_4^+ concentrations retard such reduction in pH when Pb^{2+} or Cu^{2+} concentration is lifted up. The simulated results show that under either MICP or EICP, the lower degrees of urea hydrolysis correspond to cotunnite and atacamite precipitations and also to a reduction in the immobilization efficiency (see Figures 3 and 4). Under some circumstances, the immobilization efficiency corresponding to atacamite precipitation could be as low as below 10%. In light of the above, cotunnite and atacamite's chemical stability are considered lower compared to calcite, cerussite, phosgenite, and malachite.

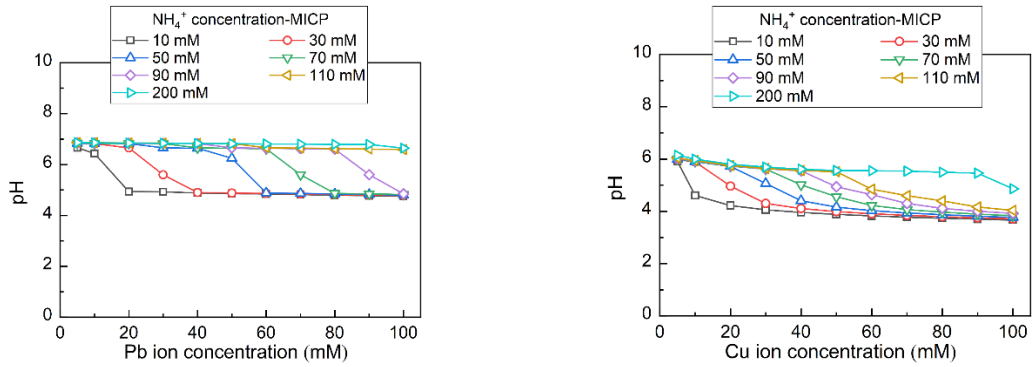


Figure 5. *(a) variations of pH surrounding against Pb^{2+} concentration under MICP and (b) variations of pH surrounding against Cu^{2+} concentration under MICP*

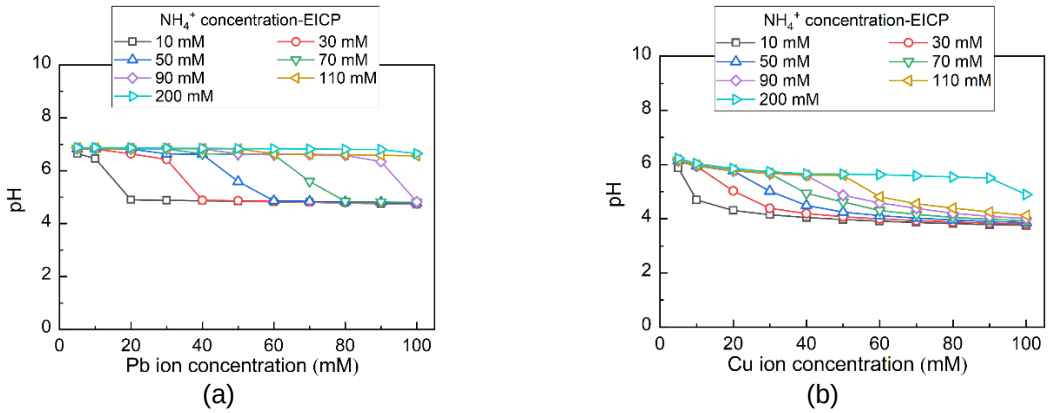


Figure 6. *(a) variations of pH surrounding against Pb^{2+} concentration under EICP and (b) variations of pH surrounding against Cu^{2+} concentration under EICP*

Given a biochemical system undergoing a reversible reaction, a thermodynamic equilibrium constant, K, is defined to be the value of the reaction quotient when forwards and reverse reactions take place at the same time. The higher the K value, the higher the transformation potential of carbonate precipitation to another phase, and the lower the thermodynamic stability. As K is linked to the standard Gibbs free energy change of reaction ΔG, their relationship can be expressed by Eq. (3).

$$\Delta G = -RT\ln K \tag{3}$$

where R represents the universal gas constant, T the absolute temperature (in Kelvins), and ln the natural logarithm. Given ΔG and R known (Benson & Teague, 1980; Robie & Hemingway, 1995; Blanc, 2017), the relationships of $\log_{10}K$ versus T (in Celsius) for the six carbonate precipitations in the simulated results are depicted in Figure 7. Amongst the six carbonate precipitations, cotunnite ($PbCl_2$) and atacamite ($Cu_2(OH)_3Cl$) are categorized as the abiotic precipitation, while calcite ($CaCO_3$), cerussite

($PbCO_3$), phosgenite ($Pb_2Cl_2CO_3$), and malachite ($Cu_2(OH)_2CO_3$) are classed as the biotic precipitation. $Log_{10}K$ for atacamite decreases from 17.16 to -0.10 when the temperature is increased from 0 to 300 deg. Further, for a given T, $log_{10}K$ for atacamite is the highest amongst the six carbonate precipitations. Moreover, the solubility product Ksp being about 7.391 for atacamite is also the highest amongst the six carbonate precipitations. The higher the Ksp, the more difficult the formation of carbonate precipitation. These results indicate that atacamite has the highest potential of transforming to another phase when subjected to a change in temperature, thus indicating a reduction in the thermodynamic stability (the lowest in the present work). On the other hand, cotunnite has the second highest Ksp, although for a given temperature, its $log_{10}K$ is the second last. Also, $log_{10}K$ for cotunnite does not show substantial change as the temperature is increased from 0 to 300 deg. Notwithstanding that, cotunnite is still considered to be unstable when such high Ksp promotes the potential of transforming to another phase during biochemical processes. These results lead us to conclude that a reduction in the immobilization efficiency could be either due to lower degrees of urea hydrolysis or to carbonate precipitation with low chemical and thermodynamic properties. Apart from that, a reduction, while remedying Cu^{2+}, could also be present due to the formation of the copper-ammonia complex.

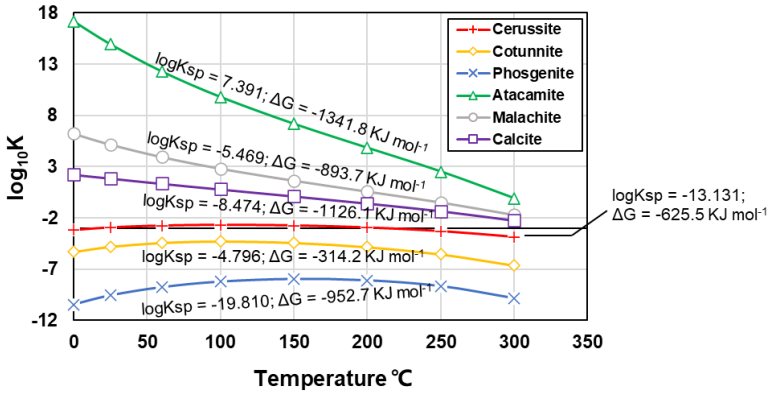


Figure 7. *Relationships of $log_{10}K$ (thermodynamic equilibrium constant) versus temperature (in Celsius) against different carbonate precipitations applied to Pb and Cu immobilization*

4 CONCLUSIONS

(1) During the biomineralization process, NH_4^+ concentration decreases when subjected to the effect of Pb^{2+} or Cu^{2+} toxicity, and for a given Pb^{2+} or Cu^{2+} concentration, it is much higher under MICP. The immobilization efficiency against Pb^{2+} using MICP performs similarly to that using EICP. However, a discrepancy in the immobilization efficiency against Cu^{2+} between MICP and EICP is observed. Further, the immobilization efficiency against Cu^{2+} is way below that against Pb^{2+}.

(2) The immobilization of Pb or Cu is attained through biotic precipitation when CO_3^{2-} concentration is high enough to precipitate the majority of Pb^{2+} or Cu^{2+}. In case CO_3^{2-} concentration is not high enough, it is attained via abiotic and biotic precipitations, corresponding to a reduction in the immobilization efficiency.

(3) The reduction in the immobilization efficiency appears to relate to the chemical and thermodynamic properties of the carbonate precipitations. Results indicate that the reduction in the immobilization efficiency is ascribed to the precipitation of cotunnite and atacamite. Their degradation may occur when subjected to harsh pH conditions or a substantial temperature change, accompanied by a reduction in the immobilization efficiency.

5 ACKNOWLEDGEMENTS

This paper is based upon work supported by the Shaanxi Educational Department (2020TD-005) and the Shaanxi Housing and Urban-Rural Development Office (2018-K15).

REFERENCES

Achal, V., Pan, X.L., Fu, Q.L., & Zhang, D.Y. (2012). Biomineralization based remediation of As(III) contaminated soil by Sporosarcina ginsengisoli. Journal of Hazardous Materials, 201: 178-184.

Aparicio, J.D., Lacalle, R.G., Artetxe, U., Urionabarrenetxea, E., Becerril, J.M., Polti, M.A., Garbisu, C., & Soto, M. (2021). Successful remediation of soils with mixed contamination of chromium and lindane: integration of biological and physico-chemical strategies. Environmental Research, 194: 110666.

Benson, L.V., & Teague, L.S. (1980). A Tabulation of Thermodynamic Data for Chemical Reactions Involving 58 Elements Common to Radioactive Waste Package Systems. Lawrence Berkeley National Laboratory, 98 p.

Blanc, P. (2017). Thermoddem: Update for the 2017 version. BGRM, 20 p.

Bhattacharya, A., Naik, S. N., & Khare, S. K. (2018). Harnessing the bio-mineralization ability of urease producing Serratia marcescens and Enterobacter cloacae EMB19 for remediation of heavy metal cadmium (II). Journal of Environmental Management, 215: 143-152.

Bzura, J., & Koncki, R. (2019). A mechanized urease activity assay. Enzym. Microb. Technol. 123, 1-7.

Castanier, S., Bernetrollande, M.C., Maurin, A., & Perthuisot, J.P. (1993). Effects ofmicrobial activity on the hydrochemistry and sedimentology of Lake Logipi, Kenya. Hydrobiologia, 267: 99-112.

Dermont, G., Bergeron, M., Mercier, G., & Richer-Lafleche, M. (2008). Soil washing for metal removal: a review of physical/chemical technologies and field applications. Journal of Hazardous Materials, 152: 1-31.

Duarte-Nass, C., Rebolledo, K., Valenzuela, T., Kopp, M., Jeison, D., Rivas, M., Azócar, L., Torres-Aravena, A., & Ciudad, G. (2020). Application of microbe-induced carbonate precipitation for copper removal from copper-enriched waters: Challenges to future industrial application. Journal of Environmental Management, 256: 109938.

Fang, L.Y., Niu, Q.J., Cheng, L., Jiang, J.X., Yu, Y.Y., Chu, J., Achal, V., & You, T.Y. (2021). Ca-mediated alleviation of Cd2+ induced toxicity and improved Cd2+ biomineralization by Sporosarcina pasteurii. Science of The Total Environment, 787: 147627.

Gat, D., Ronen, Z., & Tsesarsky, M. (2017). Long-term sustainability of microbial-induced CaCO3 precipitation in aqueous media. Chemosphere, 184: 524-531.

Gong, L., Wang, J., Abbas, T., Zhang, Q., & Di, H. (2020). Immobilization of exchangeable cd in soil using mixed amendment and its effect on soil microbial communities under Paddy upland rotation system. Chemosphere, 262: 127828.

Hamby, D.M. (1996). Site remediation techniques supporting environmental restoration activities-a review. Science of the Total Environment, 191(3): 203-224.

Jalali, M., & Khanlari, Z.V. (2007). Redistribution of fractions of zinc, cadmium, nickel, copper, and lead in contaminated calcareous soils treated with EDTA. Archives of Environmental Contamination and Toxicology, 53(4): 519-532.

Khan, F.I., Husain, T., & Hejazi, R. (2004). An overview and analysis of site remediation technologies. Journal of Environmental Management, 71 (2): 95-122.

Larsen, J., Poulsen, M., Lundgaard, T., & Agerbaek, M. (2008). Plugging of fractures in chalk reservoirs by enzyme-induced calcium carbonate precipitation. SPE Production & Operations, 23: 478-483.

Lockhart, N.C. (1983). Electro-osmotic dewatering of clay-III. Influence of clay type, exchangeable cations and electrode materials. Colloids and Surfaces, 6: 253-269.

Maubois, J. (1984). Separation, extraction and fractionation of milk protein components. Le Lait, 64: 485-495.

Mena, E., Ruiz, C., Villasñor, J., Rodrigo, M.A., & Cañizares, P. (2015). Biological permeable reactive barriers coupled with electrokinetic soilflushing for the treatment of diesel-polluted clay soil. Journal of Hazardous Materials, 283: 131-139.

Moghal, A. A. B., Lateef, M. A., Mohammed, S. A. S., Ahmad, M., Usman, A. R. A., & Almajed, A. (2020). Heavy metal immobilization studies and enhancement in geotechnical properties of cohesive soils by EICP technique. Applied Sciences, 10: 7568.

Phillips, A.J., Cunningham, A.B., Gerlach, R., Hiebert, R., Hwang, C.C., Lomans, B.P., Joseph, W., Cesar, M., Jim, Ki., Richard, E., & Lee, S. (2016). Fracture sealing with microbially-induced calcium carbonate precipitation: a field study. Environmental Science & Technology, 50: 4111-4117.

Robie, R.A., & Hemingway, B.S. (1995). Thermodynamic Properties of Minerals and Related Substances at 298.15 K and 1 Bar (105 Pascals) Pressure and at Higher Temperatures. U.S. Geological Survey, 461 p.

Wang, L., Cheng, W.C., & Xue, Z.F. (2022a). The effect of calcium source on Pb and Cu immobilization using enzyme-induced carbonate precipitation. Frontiers in Bioengineering and Biotechnology, 10: 849631.

Wang, L., Cheng, W.C., Xue, Z.F., & Hu, W.L. (2022b). Effects of the urease concentration and calcium source on enzyme-induced carbonate precipitation for lead remediation. Frontiers in Chemistry, 10: 892090.

Whiffin, V.S., van Paassen, L.A., & Harkes, M.P. (2007). Microbial carbonate precipitation as a soil improvement technique. Geomicrobiology Journal, 24: 417-423.

Xue, Z.F., Cheng, W.C., Lin, W., & Hu, W.L. (2022). Effects of bacterial inoculation and calcium source on microbial-induced carbonate precipitation for lead remediation. Journal of Hazardous Materials, 426: 128090.

Zhu, Z., Wang, J., Liu, X., Yuan, L., Liu, X., & Deng, H. (2021). Comparative study on washing effects of different washing agents and conditions on heavy metal contaminated soil. Surfaces and Interfaces, 27: 101563.

Zine, H., Midhat, L., Hakkou, R., El Adnani, M., & Ouhammou, A. (2020). Guidelines for a phytomanagement plan by the phytostabilization of mining wastes. Scientific African, 10: e00654.